A benchtop Single-Sided magnet with NMR well-logging tool specifications – Examples of application

Rodrigo de Oliveira-Silva[1], Éverton Lucas-Oliveira[2], Arthur Gustavo Araújo-Ferreira[2], Willian Andrighetto Trevizan[3], Edson Luiz Géa Vidoto[2], Dimitrios Sakellariou[1]*, Tito José Bonagamba[2†]

[1]*Centre for Membrane Separations, Adsorption, Catalysis and Spectroscopy for Sustainable Solutions (cMACS), Department of Microbial and Molecular Systems (M2S), KU Leuven, Leuven, Belgium.*

[2]*São Carlos Physics Institute, University of São Paulo, São Carlos – SP, Brazil.*

[3]*Cenpes, Petrobras Research Center, Rio de Janeiro – RJ, Brazil.*

corresponding authors: *dimitrios.sakellariou@kuleuven.be, †tito@ifsc.usp.br

Abstract

This article was written in honor of Prof. Bernhard Blümich, who has heavily impacted many areas of Magnetic Resonance and, in particular, low-field and portable NMR with numerous advances, concepts, innovations, and applications of this impressive technology. Many years ago, we decided to research and develop single-sided magnets for the area of petroleum science and engineering to study oil reservoir rocks in the laboratory under well-logging conditions. The global urge to exploit oil reserves requires the analysis of reservoirs, intending to characterize the yields before starting the production. Thus, well-logging tools have been developed to estimate the quality of oil and reservoir productivity. NMR logging is included in these analytical tools, and numerous operations using this kind of device were performed since the early 1950s. To contribute to this vital research area, we show the development of a new benchtop single-sided NMR system, with well-logging tool characteristics, a cylindrical sweet spot with 4 cm of diameter and length, with magnetic field of 47 mT centered at 11 cm from the magnet's surface and a linear gradient of 35.7 G/cm along z. This system was used in self-diffusion, T_1-T_2, and D-T_2 measurements of standard liquids and rock cores, demonstrating its functionality.

Keywords: Single-sided magnet, NMR well-logging, deep sweet spot, NMR porous media.

Introduction

Fossil-based fuels and petrochemicals are still essential for the global economy. Due to the high demand for fossil fuels, the number of operations dedicated to finding and exploiting petroleum reserves onshore and offshore has grown intensely in recent years. That creates the need for exploring reservoirs in challenging environments such as deep water, or unconventional resources like shale oil and gas, to serve global demand.[1] Therefore, existing physical methods are being improved, and new ones developed to find new oil reservoirs and enhance their production. One of the most important and traditional physical methods employed for the analysis of oil embedded rock formations is Nuclear Magnetic Resonance (NMR), which is used in laboratory research and well-logging operations.[2,3]

Throughout the years, NMR tools have been used to assist the estimations of reservoirs porosity, permeability and fluid typing. Nowadays, an effort is being made to increase the accuracy of NMR Logging While Drilling (LWD) acquisition,[4] where the rotation of the tool following the drill bit imposes the necessity of understanding the acquisition under a somewhat erratic motion. Our research groups are fully dedicated to developing new NMR methods and instrumentation for both scenarios. In the case of NMR spectrometers employing traditional magnets, several contributions were already given[5–16]. Currently, substantial efforts have been dedicated to developing single-sided magnets, as well as NMR methods and studies under simulated reservoir conditions.

NMR well-logging was one of the first industrial NMR applications, starting in the 1950s. Since then, it has continually evolved, reaching a prominent position among the most used techniques for profiling oil reservoirs, making it an indispensable tool for the petroleum industry.[17] New magnets used for NMR well-logging are continuously designed to generate a relatively strong magnetic field inside the rock formations, having a specific profile within a so-called “sweet spot” volume. That is why this class of magnets was called “single-sided” or “inside-out”.[18] Complementarily, appropriate radio-frequency (rf) surface coils are also designed for use with the single-sided magnets to excite and detect nuclear spins at the sweet-spot. Using these distinctive magnets and rf coils, it is possible, for example, to study liquids confined in an oil reservoir rock and estimate the permeability.[3] However, such single-sided NMR sensors are not limited only to the oil industry, and several other applications have already been proposed.[19–22]

The term inside-out NMR was coined early in the well logging prospection literature,[23] and different designs of well logging tools have been since proposed.[17] Well logging tools from different oil companies have different designs, e.g., NUMAR/Halliburton's well logging NMR tool MRIL (Magnetic Resonance Imaging Logging-Prime) and Schlumberger's tool PNMT (Pulse Nuclear Magnetism Tool).[24,25] The former measures cylindrical shells to the borehole, with ^{1}H frequencies between 580 kHz to 760 kHz, depending on the depth, with a magnetic field gradient of 25 G/cm, while the latter measures a localized volume in the rock formation, with a ^{1}H frequency of about 2 MHz.[25,26] Additional considerations, such as the temperature of operation, usually much higher than room temperature, are taken into account for the choice of the magnetic materials.

A large variety of small transportable single-sided systems have been developed.[27–30] These systems can have magnetic fields parallel,[27] or perpendicular[28–30] to the magnet surface, and produce either homogeneous magnetic fields, or magnetic field gradients inside the sweet spot.

Generating purely linear gradients over large regions of space is interesting both for imaging and diffusion measurements, but it proves to be impossible at low magnetic fields because of the presence of concomitant gradient components. However, theoretical analysis using spherical harmonics demonstrates that it is possible to make homogeneous magnetic fields on the XY plane located at a certain distance from the magnet while having a homogeneous gradient on the Z-axis. This methodology has already been successfully applied to design a single-sided system capable of generating a sweet spot with a 0.3 T magnetic field and a 340 G/cm magnetic field gradient, at 2 cm from the surface of the magnet.[28,31] This system was used to measure self-diffusion in thin samples and to perform multimodal experiments with a Small Angle Neutron Scattering (SANS).[32–34] Using the same principles, a new single-sided system was designed and built, presenting magnetic field specifications appropriate for well-logging applications, including a sizeable sweet spot located at a considerable distance from the magnet surface.

This paper presents the developments of this novel single-sided NMR system having well-logging tool specifications and the first NMR experiments performed with water-embedded porous media, including distribution of transverse relaxation times (T_2) and diffusion coefficients (D), as well as two-dimensional correlation maps DxT_2 and T_1xT_2.

Experimental

Magnet Development

The target specifications for the built single-sided magnet were 470 G in magnetic field strength and 30 G/cm constant gradient over a 36 mm diameter spherical volume located at a significant distance (>10 cm) from its surface. The magnetic field direction has been specified to be perpendicular to the magnet's surface in order to generate the sweet spot at a greater distance from its surface. As suggested in many literature references[30,31,35,36], a cylindrical geometry was chosen, generating a cylindrically shaped sweet-spot, see Figure 1, and the Spherical Harmonic Decomposition theoretical framework was employed for the calculations[28,31]. The dimensions of the magnet (thickness, inner and outer diameter) were optimized using analytical formulas to achieve the required specifications. Because of the flat shape of the magnet, these numerical results were further optimized using a 3D finite element software (Radia) where the effects of demagnetization were properly accounted for (using the susceptibility properties of the material) and the dimensions were slightly corrected before fabrication. Since the magnet's operation would take place in the laboratory at room temperatures, NdFeB magnetic material (grade N48SH) was purchased (The RE Magnet Studio Ltd.), instead of SmCo, which is typically used in well logging NMR sensors.

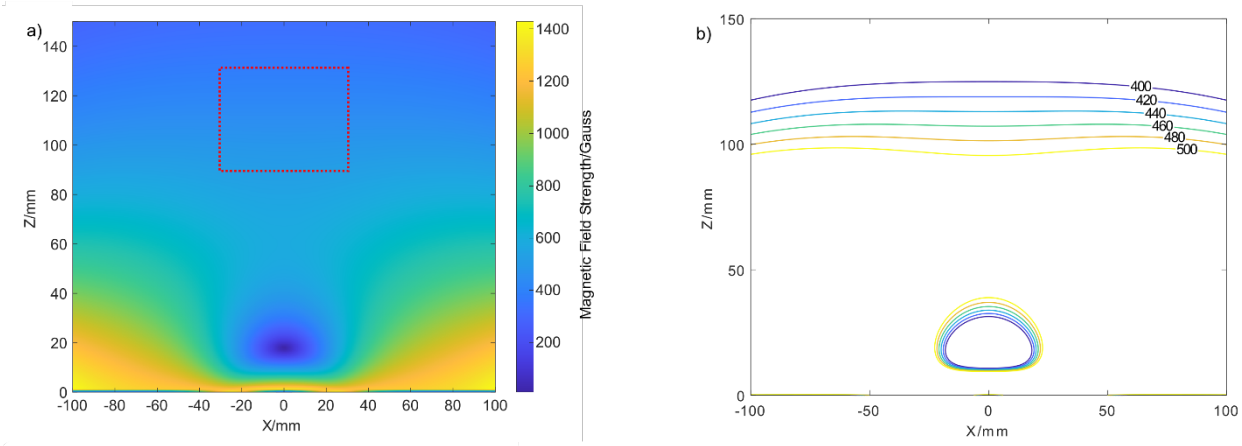

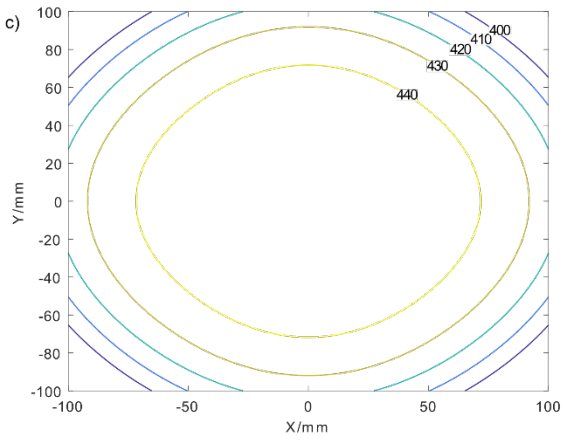

Figure 1 – Magnetic field design characteristics. In a) the simulated magnetic field map in the XZ plane is shown. The red dashed line rectangle corresponds to a cross section of the cylindrical sweet spot volume. Figure b) contour lines in the same region are highlighting the intensity of the magnetic field between 400 and 500 Gauss. c) Surface plot of the magnetic field strength in the XY plane calculated at the sweet spot location 11 cm from the surface of the magnet.

The pieces were glued inside a disk-shaped aluminum frame, as shown in Figure 2(a). The magnet's height and diameter were 45 mm and 374 mm, respectively. Because of its large size (~40 kg in weight), mounting magnetized pieces would represent a hazard and would not guarantee uniformity of magnetization. For this reason, the entire assembly was magnetized after mounting and gluing it in a non-magnetized state. The magnetization took place at the LNCMI facility (Grenoble / France). After magnetization, its magnetic field was roughly mapped using a SENIS 3MH3-20T 3-axis Hall probe. The resolution of this probe (10G) does not allow very precise magnetic field measurements but it allows a quick assessment of the magnetic field profile of the magnet. The measured magnetic field orientation was perpendicular to its surface, and its magnitude along the Z-axis is plotted in Figure 2b. The field on-axis shows a flat maximum (having some homogeneity) at 70 mm from the surface and then decays mainly linearly along the Z-axis. The constant gradient sweet spot's location lies 11 cm from its surface, where the nominal field magnitude is (470 ± 10) G and the measured gradient (33 ± 5) G/cm. At this vertical position, mapping the magnitude of the field in the XY-plane, as shown in Figure 2c, demonstrates the excellent field uniformity over at least 50 mm in diameter.

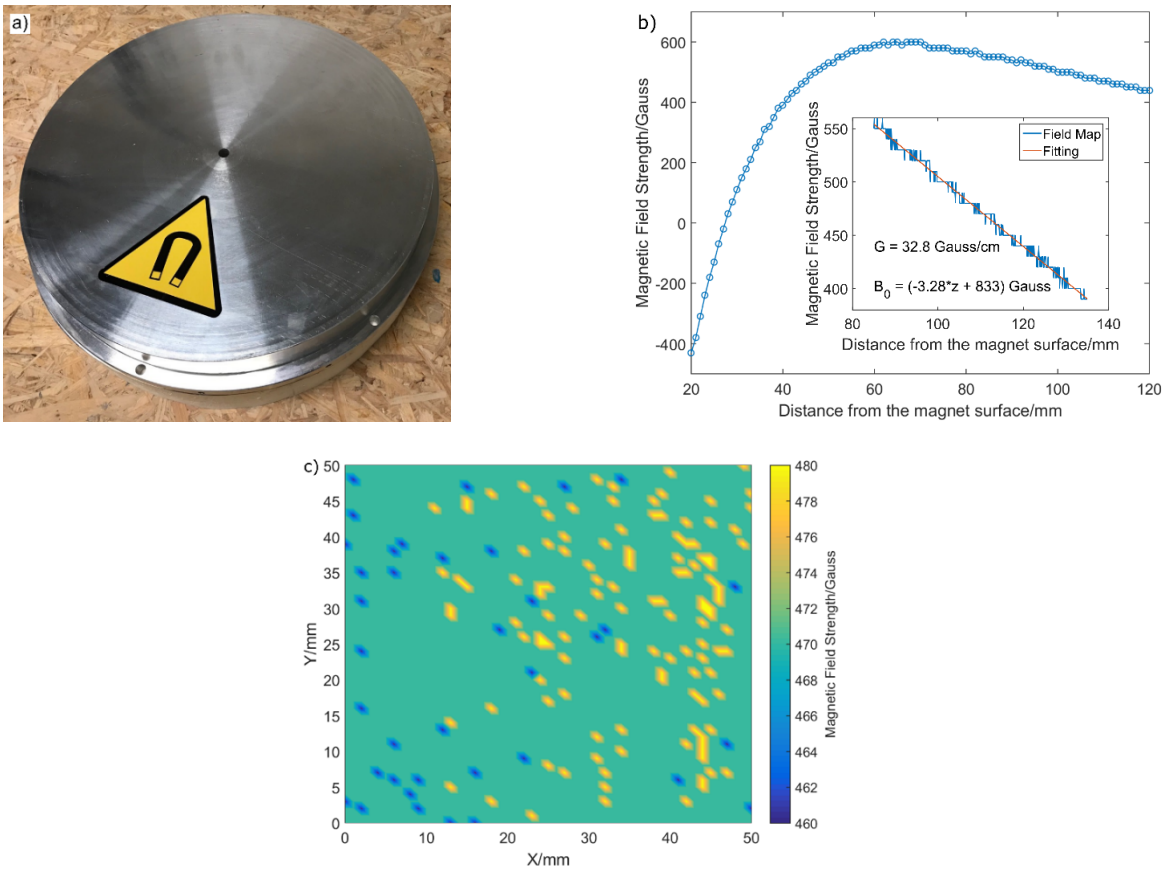

Figure 2 – Single-sided benchtop well-logging magnet. (a) Photograph of the permanent magnet assembly (total dimensions: 40 cm diameter, 5.5 cm height, 40 kg weight). (b) Magnetic field profile along the z-axis (perpendicular to the surface of the magnet), measured using a Hall probe. The magnetic field intensity at the sweet spot (11 cm) is (470 ± 10) G and magnetic field gradient (33 ± 5) G/cm. (c) Magnetic field profile in the XY-plane (parallel to the surface of the magnet), measured using a Hall probe at the location of the sweet spot.

Probes

Two NMR probes were designed and constructed for the measurements using the single-sided magnet, both operating at 2 MHz (^{1}H Larmor frequency), the respective coils are shown in the Figure 3. The first one has a solenoid coil with 26 turns, a diameter of 48 mm, and a length of 53 mm, which can accommodate cylindrical samples with a maximum diameter of 44 mm. Its purpose is testing the sensitivity over a specific region by using a homogeneous B_1 field. The second one has an eight-shaped planar surface coil, to attain a sensitive region outside the probe, which will not limit the shape of the sample to be studied. The planar eight-shape coil expands over an area 180 mm long and 80 mm wide.

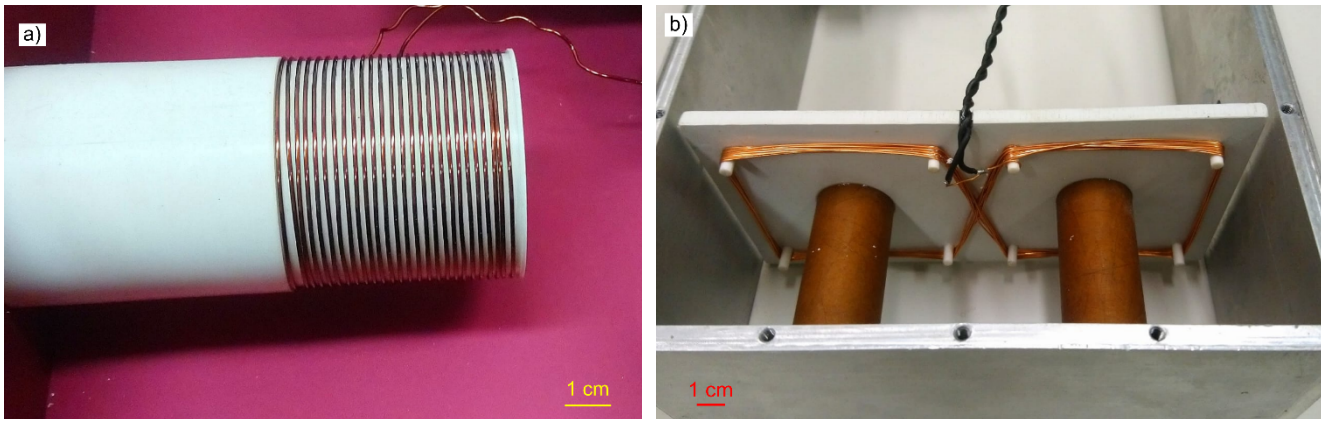

Figure 3 – Coils used for the measurements. a) Solenoid coil with 26 turns, 53 mm of length and 48 mm of diameter and b) eight-shape coil mounted under a PVC support, with 9 turns and dimensions 180 mm in length and depth of 80 mm. The sample is placed at the region above the support to be measured.

Both probes have the same rf circuit topologies, a simple conventional dual capacitor in association with the sample coil.[37] A parallel capacitor with the sample coil adjusts the resonance frequency, and a series capacitor adjusts the 50-ohm matching. Both solenoidal and surface coils were designed to have low quality factors Q of 12 and 22, respectively, to reduce the ringing time and enable shorter rf hard-pulses, which is desirable because of the intense magnetic field gradient. The simulated and measured sensitivity of the solenoidal probe are 4.7 G/Amp and 4.6 G/Amp, respectively. Table 1 summarizes the sensitivity of the eight-shaped planar coil for different distances from its surface.

Table 1 – Simulated and measured sensitivities of the eight-shaped planar coil for different distances from its surface.

Distance (mm)	Simulated Sensitivity (G/Amp)	Measured Sensitivity (G/Amp)
5	7.6	--
10	3.6	3.5
20	1.6	1.6
30	0.8	0.9

The probe coils were made by winding enameled copper wire around rigid PVC mechanical supports. Variable non-magnetic Polyflon capacitors (5-125 pF, 6 kV) were used for tuning and an association of fixed value porcelain ATC capacitors (model 100E) for matching. The Q damping was provided with the association of a non-inductive, non-magnetic, power Vishay resistor. Both probes were assembled inside aluminum boxes with 4 mm thick walls to provide electromagnetic shielding and mechanical stability.

Samples

For the evaluation of the single-sided system, different samples were used. Self-diffusion experiments were performed with bulk water, methanol, ethanol, and acetone. T_1-T_2

experiments were performed with Berea and Indiana rock cores 38 mm in diameter and length, and also with bulk water and mineral oil samples placed in the same sample holder but separated in different tubes. D-T_2 experiments were also performed with the two rock cores.

NMR Experiments

A Tecmag NMR console (LapNMR) in association with a Tomco rf power amplifier (BT00500-AlphaS) were used to perform the single-sided NMR experiments. The widths for the 90° excitation pulses were 7 μs and 9 μs, for the solenoid and eight-shape coil probes, respectively. Furthermore, the 180° pulse length was set to twice those values. The temperatures of the magnet, probes and samples were kept constant at (25.0 ± 0.1)°C during the experiments.

For the solenoid coil, with a diameter of 48 mm, despite providing good B_1 field homogeneity, there is a B_0 variation of 144 G along its diameter and, consequently, a Larmor frequency distribution of about 600 kHz along the z-axis, due to the magnetic field gradient of ~33 G/cm. The 90° and 180° rf pulses are however selective due to their durations of 7 μs and 14 μs, resulting in excitation bandwidths of approximately 140 kHz and 70 kHz, respectively. A bandwidth of 70 kHz corresponds to an excited slice of ~5 mm.

Similarly, for the eight-shaped coil, the B_0 gradient determines that only part of the sample will be excited. However, in addition to the B_0 gradient, the B_1 magnetic field produced by this coil has a non-uniform profile. That modifies further the shape of the excited region of the sample. The losses in the S/N ratio due to the employed RF pulses' selectivity were compensated by the number of averages of the experiments.

Self-diffusion, T_1-T_2, and D-T_2 were performed with the standard CPMG acquisition, with echo time $2t_e = 200\ \mu s$ (see Figure 4). Two dimensional T_1-T_2 relaxation time correlations[37] were measured using the inversion recovery experiment, for the encoding of T_1 with 16 recovery times t_1 logarithmically spaced from 100 μs to 10 s (Figure 4a). Additionally, 8000 echoes were measured in the T_2 decay for the Indiana and the water/oil samples and 4000 echoes for the Berea sample. The self-diffusion and D-T_2 experiments were performed according to the pulse sequence presented in Figure 4b.[38,39] Furthermore, for self-diffusion experiments performed with the bulk liquids, the sum of the 100 first echoes was used to improve the signal to noise ratio, since the T_1 relaxation times are on the order of seconds. For self-diffusion experiments with rocks, the full decay was measured comprising 8000 echoes and 4000 echoes, respectively, for the Indiana and Berea samples. The diffusion encoding times t_d ranged from

564 µs to 6 ms in 10 equidistant steps in t_d^3 domain. The number of averages are summarized in the Table 2.

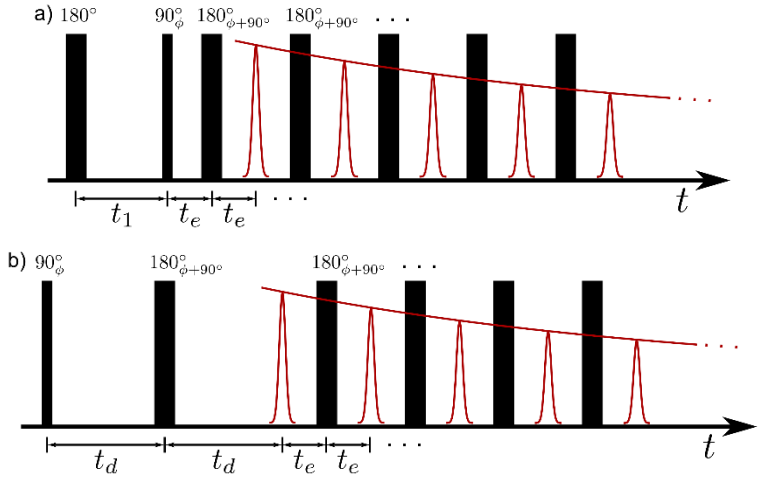

Figure 4 – (a) The T_1-T_2 correlation experiment is performed by combining the IR and CPMG experiments. The T_1 modulated signal intensity (because of the different recovery time t_1 between the 180° and the 90° pulses) is measured with the CPMG sequence, consisting of a train of echoes separated by two times t_e.[37] (b) Similarly, the D-T_2 correlation experiment measures the T_2 relaxation while encoding the diffusion time's (t_d) effect on the signal intensity.[38,39]

Table 2 – Number of averages of the performed experiments.

Sample	Self-Diffusion	D-T_2	T_1-T_2
Berea	NA	128	128
Indiana	NA	128	128
H_2O + Oil	NA	NA	128
H_2O	16	NA	NA
Acetone	16	NA	NA
Methanol	32	NA	NA
Ethanol	16	NA	NA

NA = not applicable.

Data processing

In general, two-dimensional NMR sequences based on the relaxation process are formulated with the aim of being represented by two independent *kernels*. Thus, the measured magnetization $M(y_1, y_2)$ can be written as:[37–39]

$$M(y_1, y_2) = \iint dx_1 dx_2 f(x_1, x_2) k_1(x_1, y_1) k_2(x_2, y_2) + \epsilon(y_1, y_2) \quad (1)$$

where $f(x_1, x_2)$ is the distribution function of interest, and k_1 and k_2 are the kernels related to the kind of experiment. Based on the sequences shown in Figure 4, the kernels are given by:

$$k_1^{T_1T_2}(T_1, t_1) = 1 - 2\exp\left(-\frac{t_1}{T_1}\right), \quad (2)$$

$$k_1^{DT_2}(D, 2t_d) = \exp\left(-\frac{2}{3}\gamma^2 G^2 D t_d^3\right)\exp\left(-\frac{2t_d}{T_2}\right), \quad (3)$$

$$k_2(T_2, Nt_e) = \exp\left(-\frac{Nt_e}{T_2}\right), \quad (4)$$

where k_2 is the same for all sequences, based on the standard CPMG with N echoes, γ is the gyromagnetic factor, G is the gradient and D the self-diffusion coefficient. T_1-T_2 kernel (k_1^{T1T2}) and formulation are the same used by Song *et al.*,[37] for the fast 2D Laplace Inversion transform (2D – ILT) algorithm.[37] Thus, based on this algorithm, an Octave script was developed to process T_1-T_2 experiment data.

On the other hand, the kernel for the diffusion-editing proposed by Hürlimann *et al.*[38] rewrites the kernel $k_1^{DT_2}$. The approach was made so that the fast 2D Laplace Inversion transform should be applied. In this case, the algorithm was implemented, considering the $k_1^{DT_2}$ without approximation, making data processing slower, which, for the purpose of this work, has no implications.

The self-diffusion coefficients for the bulk-liquids where determined by the fitting with exponential model according to equation (5):[32]

$$I(2t_d) = I_0 \exp\left(-\frac{2t_d}{T_2^*} - \frac{2}{3}\gamma^2 G^2 t_d^3 D\right), \quad (5)$$

where $I(t)$ are the signal intensities corresponding to each of the t_d values. Thus, I_0 is the signal intensity for the initial t_d value, T_2^* corresponds to the transverse magnetization attenuation constant between the periods t_d (according to the Figure 4b), γ is the gyromagnetic factor, G is the gradient and D the self-diffusion coefficient to be determined by the fitting.

Results

To measure the magnetic field gradient at the sweet spot, five consecutive self-diffusion NMR experiments were performed for bulk-water at 25°C using the solenoid probe. The magnetic field gradient was estimated for each experiment according to the equation (5) to match the well-established self-diffusion coefficient of water at 25°C of 2.299 x 10^{-5} cm^2s^{-1}.[40] Results are presented in Table 3.

Table 3 - Sweet spot magnetic field gradient estimated with the bulk water diffusion coefficient at 25ºC.

Experiment number	1	2	3	4	5	Average
G (G/cm)	35.43	35.60	35.84	36.33	35.67	35.7 ± 0.3

The average magnetic field measured by NMR (Table 3) is (35.7 ± 0.3) G/cm, which is in the same range of that obtained by Hall probe. Table 4 summarizes the measured self-diffusion coefficients for four fluids at 25°C, including water, which are in accordance with the self-diffusion established in the literature,[40,41] corroborating the value of the measured magnetic field gradient.

Table 4 – Self-diffusion coefficients measured using the single-sided magnetic field gradient. The self-diffusion experiments were repeated *n* times for each sample, and the standard deviation calculated.

Bulk liquid	*n*	*D* (x$10^{-5}$$cm^2s^{-1}$)(Literature)	*D* (x$10^{-5}$$cm^2s^{-1}$)(Measured)
Water	5	2.299	2.31 ± 0.04
Methanol	5	2.41	2.5 ± 0.2
Ethanol	4	1.07	1.1 ± 0.1
Acetone	2	4.57	4.5 ± 0.8

T_1-T_2 correlation experiments were performed for water-saturated Berea sandstone and Indiana limestone rocks, as well as a phantom composed of two glass tubes containing, separately, a 5-mM aqueous copper sulfate solution and mineral oil. The experiments were carried out using the eight-shaped probe, with the sample on top of the platform and centered on the sweet spot. The corresponding T_1-T_2 maps are presented in Figure 5. For the three samples, one can observe the tendency of the distributions to be parallel to the main diagonal (white dash-line where T_1=T_2).

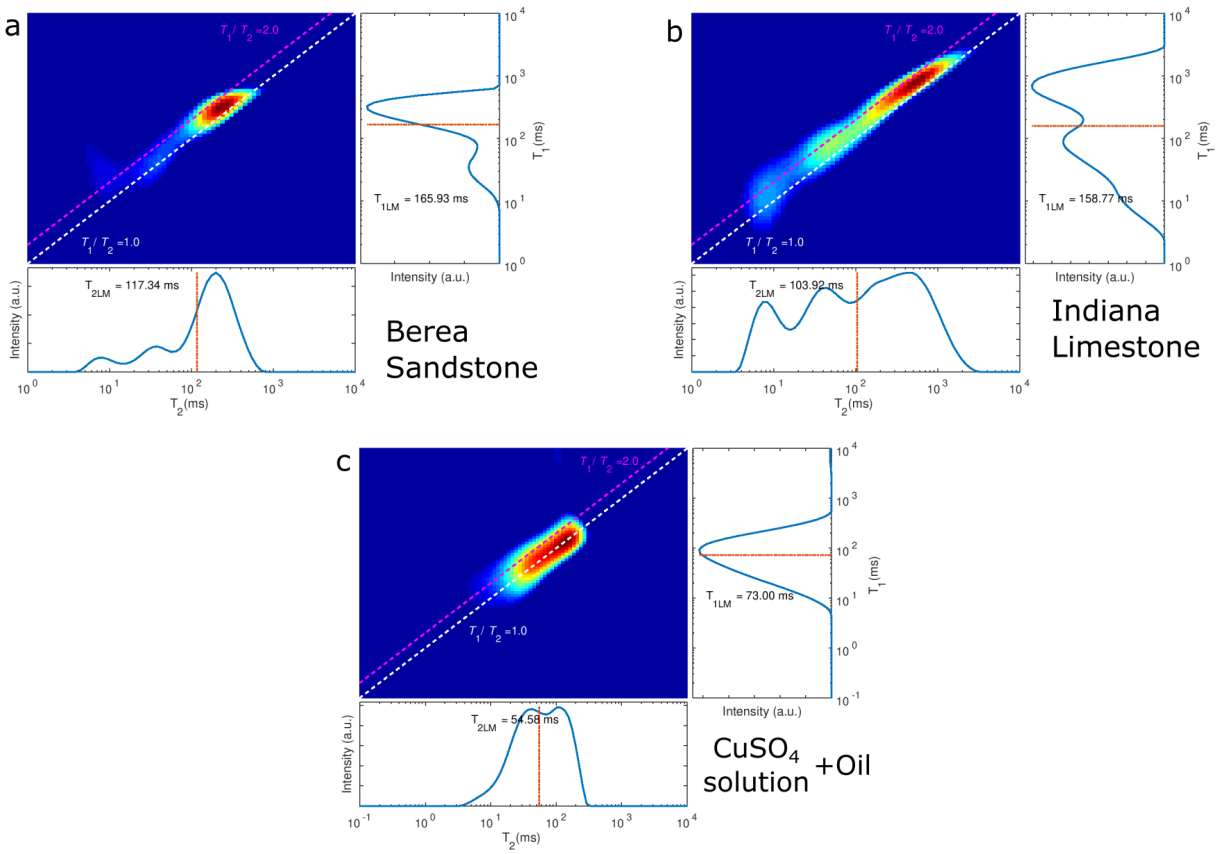

Figure 5 – T_1-T_2 maps obtained on the single-sided magnet using the eight-shape probe for: a) Berea sandstone, b) Indiana limestone, and c) 5-mM aqueous CuSO4 solution and mineral oil.

It is known that for water and light oil, the relaxation time T_2 tends to be close to T_1, as observed in the T_1-T_2 distribution, which shows the distribution overlapping the white dashed-line[2]. In the case of the water saturating rocks, the fast diffusion regime ensures that the T_1 and T_2 are proportional to the pore sizes.[42,43]

Recently, Lucas-Oliveira *et al.*[6] evaluated 14 sandstones, including the same Berea sandstone used in this work. On that work, they measured the relaxation time in a conventional 0.047 T

magnet, which presented the same shape shown in Figure 5a, and, for both cases, the longest T_2 are ~200 ms. Additionally, the parallel behaviour obtained by the T_1-T_2 maps results shown here, indicates that the surface relaxivity, estimated by Lucas-Oliveira *et al.*, could be considered uniform for all the pores, presenting the same interactions between the water and pore surfaces. Indiana limestone showed similar behaviour and a wide T_2 distribution, which indicates a wide pore size distribution as well.

D-T_2 experiments were performed for both Berea and Indiana samples with the solenoid probe, results are shown in Figure 6. The T_2 projections are in the same range of the T_2 projections shown in Figure 5. In this case, the diffusion coefficient is related to the restriction imposed by the pore structure, which is directly related to the size and connectivity of the pores.[44,45] Given that, the water diffusion coefficient for water saturated Berea and Indiana Limestone showed to be slightly smaller than the bulk water. Additionally, the T_2 distribution appears to be shifted to shorter times, especially for the Indiana limestone, which suggests a contribution from the magnet gradient on the relaxation. Hürlimann *et al.*[38] showed that the Diffusion-editing technique measures not the D-T_2 correlations, but D-T_{2eff} correlation. That is because, in the off resonance nuclei, the measured relaxation time (T_{2eff}) is affected by a combination of T_2 and T_1.

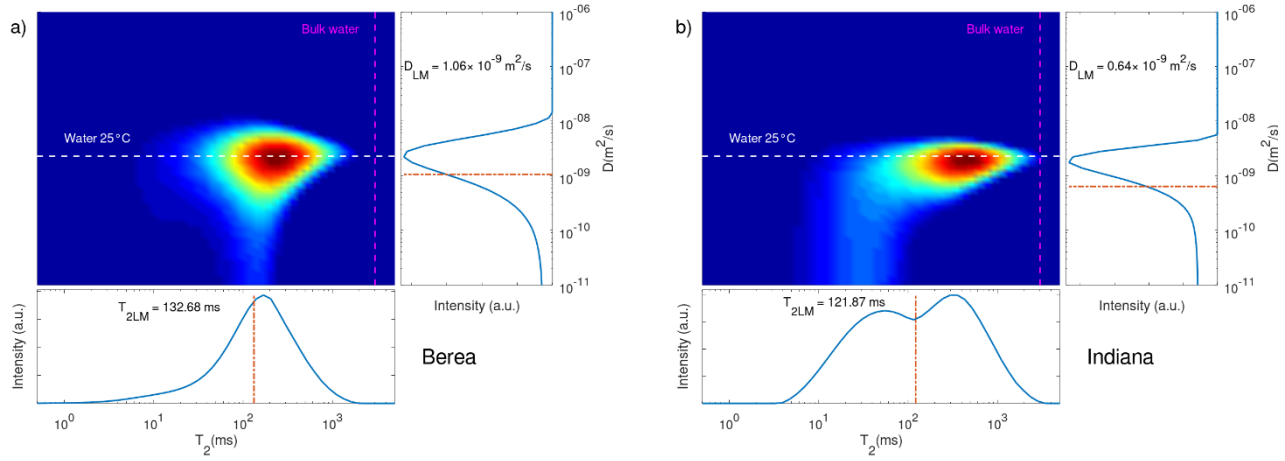

Figure 6 – D-T_2 2D distributions obtained for: a) Berea sandstone and b) Indiana limestone with the solenoid probe.

Conclusions

This work shows the first results obtained with a novel single-sided NMR sensor, designed with magnetic specifications similar to those used for well-logging tools. The characteristics of this new benchtop single-sided magnet are due to the design and manufacturing methods

proposed. The Hall probe field mapping showed that the desired sweet spot of 4 cm in diameter, with central frequency of 2 MHz and a constant magnetic field gradient of (33 ± 5) G/cm, is located 11 cm from the magnet surface. NMR also obtained similar parameters. With surface and solenoid coils, experiments were performed to evaluate the magnet performance. Self-diffusion experiments performed on bulk water at 25°C showed that the gradient in the sweet spot is (35.7 ± 0.3) G/cm, which is in the same range of that obtained by Hall probe. This gradient was used to measure the self-diffusion of other bulk liquids, and compare them to the literature values.[40,41] The D-T_2 correlation, measured on two standard rocks, presented broad diffusion coefficients distributions, close to the bulk water diffusion values. T_1-T_2 correlation, as expected for rocks and liquids in bulk, presented diagonal distributions, giving T_2 proportional to T_1. Altogether, results show the system's reliability in the development of methods and the study of fluids in porous materials to be applied in well logging applications, with the advantage of being a lower cost and safer solution than stray field measurements from superconducting magnets. In addition, this system is more flexible, enabling to emulate reservoir conditions in the lab, such as controlled sample temperature and pressure, and even acquisitions with relative motion between the sample and the magnet. This single-sided NMR equipment is already being used for developing pulse sequences for well-logging applications, including high pressure / temperature studies and measurements under logging while drilling (LWD) conditions.[4] Although this NMR equipment was originally built for applications in petroleum science and engineering, it may also find uses in many other areas, such as in industry, agriculture and medicine.

Acknowledgements

Authors acknowledge the support of the following Institutions: Universidade de São Paulo (USP), Brazil; Centro de Pesquisa e Desenvolvimento Leopoldo Américo Miguez de Mello (Cenpes), Brazil, 2012/00380-5; and Fundação de Amparo à Pesquisa do Estado de São Paulo (FAPESP), Brazil, 2009/54880-6. E. Lucas-Oliveira acknowledges Conselho Nacional de Desenvolvimento Científico e Tecnológico (CNPq), Brazil, 140215/2015-8. T. J. Bonagamba acknowledges CNPq, Brazil, 308076/2018-4. Authors also acknowledge Aparecido D. F. de Amorim for designing and assembling the NMR probes and Vinicius de França Machado for his full support. This work was also supported by the Research Foundation Flanders (FWO) under Grant PorMedNMR nr. G0D5419N and from LNCMI-CNRS, member of the European Magnetic Field Laboratory (EMFL).

References

(1) Shoeder, D. J.; Borglum, S. J. *The Fossil Fuel Revolution: Shale Gas and Tight Oil*; Elsevier, 2019. https://doi.org/10.1016/B978-0-12-815397-0.01001-6.

(2) Coates, G.; Xiao, L.; Prammer, M. *NMR Logging: Principles and Applications*, 1st ed.; Halliburton Energy Services Publication: Houston, 1999.

(3) Dunn, K.-J.; Bergman, D. J.; Latorraca, G. A. *Handbook of Geophysical Exploration. Seismic Exploration. Nuclear Magnetic Resonance Petrophysical and Logging Applications.*, 1st ed.; Pergamon: London, 2002.

(4) Coman, R.; Thern, H.; Kischkat, T. Lateral-Motion Correction of NMR Logging-While-Drilling Data. In *SPWLA-2018-LLL*; Society of Petrophysicists and Well-Log Analysts: SPWLA, 2018; p 13.

(5) Jácomo, M. H.; Trindade, R. I. F.; Lucas-Oliveira, E.; Bonagamba, T. J. Magnetic Matrix Effects on NMR Relaxation Times in Sandstones: A Case Study in Solimões Basin. *Journal of Applied Geophysics* **2020**, 104081. https://doi.org/10.1016/j.jappgeo.2020.104081.

(6) Lucas-Oliveira, E.; Araujo-Ferreira, A. G.; Trevizan, W. A.; Coutinho dos Santos, B. C.; Bonagamba, T. J. Sandstone Surface Relaxivity Determined by NMR T2 Distribution and Digital Rock Simulation for Permeability Evaluation. *Journal of Petroleum Science and Engineering* **2020**, *193*, 107400. https://doi.org/10.1016/j.petrol.2020.107400.

(7) Montrazi, E. T.; Monaretto, T.; Bonagamba, T. J.; Colnago, L. A. New and Rapid Pulse Sequences for Two-Dimensional D-T1 Correlation Measurements. *Journal of Magnetic Resonance* **2020**, *315*, 106749. https://doi.org/10.1016/j.jmr.2020.106749.

(8) Barsi-Andreeta, M.; Lucas-Oliveira, E.; de Araujo-Ferreira, A. G.; Trevizan, W. A.; Bonagamba, T. J. Pore Network and Medial Axis Simultaneous Extraction through Maximal Ball Algorithm. *arXiv:1912.04759 [physics]* **2019**.

(9) Montrazi, E. T.; Bonagamba, T. J. Direct NMR T1 Distribution Measurement without Using Ill-Posed Fitting Methods. *Journal of Magnetic Resonance* **2019**, *309*, 106624. https://doi.org/10.1016/j.jmr.2019.106624.

(10) Jácomo, M. H.; Trindade, R. I. F.; French, M.; Lucas-Oliveira, É.; Montrazi, E. T.; Bonagamba, T. J. Nuclear Magnetic Resonance Characterization of Porosity-Preserving Microcrystalline Quartz Coatings in Fontainebleau Sandstones. *Bulletin* **2019**, *103* (9), 2117–2137. https://doi.org/10.1306/01301918104.

(11) Montrazi, E. T.; Bonagamba, T. J. Saturation-Recovery as a T1-Filter for T2-T2 Exchange NMR. *Journal of Magnetic Resonance* **2019**, *301*, 67–72. https://doi.org/10.1016/j.jmr.2019.03.001.

(12) Lucas-Oliveira, E.; Araujo-Ferreira, A. G.; Trevizan, W. A.; Fortulan, C. A.; Bonagamba, T. J. Computational Approach to Integrate 3D X-Ray Microtomography and NMR Data. *Journal of Magnetic Resonance* **2018**, *292*, 16–24. https://doi.org/10.1016/j.jmr.2018.05.001.

(13) Jácomo, M. H.; Trindade, R. I. F.; de Oliveira, E. L.; Leite, C. de M. M.; Montrazi, E. T.; Andreeta, M.; Bonagamba, T. J. Nuclear Magnetic Resonance and Pore Coupling in Clay-Coated Sandstones With Anomalous Porosity Preservation, Água Grande Formation, Recôncavo Basin, Brazil. *Petrophysics* **2018**, *59* (02), 136–152.

(14) Montrazi, E. T.; Lucas-Oliveira, E.; Araujo-Ferreira, A. G.; Barsi-Andreeta, M.; Bonagamba, T. J. Simultaneous Acquisition for T 2 - T 2 Exchange and T 1 - T 2 Correlation NMR Experiments. *Journal of Magnetic Resonance* **2018**, *289*, 63–71. https://doi.org/10.1016/j.jmr.2018.02.008.

(15) D'Eurydice, M. N.; Montrazi, E. T.; Fortulan, C. A.; Bonagamba, T. J. T2-Filtered T2-T2 Exchange NMR. *Journal of Chemical Physics* **2016**, *144* (20). https://doi.org/10.1063/1.4951712.
(16) Krebs, M.; Lungwitz, B.; Souza, A.; Pépin, A.; Montoya, S.; Schlicht, P.; Boyd, A.; Vidoto, E.; Polli, R.; Bonagamba, T. The First Visualization of Acid Treatments on Carbonates With 3D Nuclear-Magnetic-Resonance Imaging. *SPE Journal* **2015**, *20* (04), 678–688. https://doi.org/10.2118/168198-PA.
(17) Kleinberg, R. L.; Jackson, J. A. An Introduction to the History of NMR Well Logging. *Concepts Magn. Reson.* **2001**, *13* (6), 340–342. https://doi.org/10.1002/cmr.1018.
(18) Jackson, J. A.; Burnett, L. J.; Harmon, J. F. Remote (inside-out) NMR. III. Detection of Nuclear Magnetic Resonance in a Remotely Produced Region of Homogeneous Magnetic Field. *Journal of Magnetic Resonance (1969)* **1980**, *41* (3), 411–421. https://doi.org/10.1016/0022-2364(80)90298-X.
(19) Blümich, B.; Perlo, J.; Casanova, F. Mobile Single-Sided NMR. *Progress in Nuclear Magnetic Resonance Spectroscopy* **2008**, *52* (4), 197–269. https://doi.org/10.1016/j.pnmrs.2007.10.002.
(20) Casanova, F.; Perlo, J.; Blümich, B. *Single-Sided NMR*; Springer: Berlin, Heidelberg, 2011; Vol. 1. https://doi.org/10.1007/978-3-642-16307-4.
(21) Danieli, E.; Blümich, B. Single-Sided Magnetic Resonance Profiling in Biological and Materials Science. *Journal of Magnetic Resonance* **2013**, *229*, 142–154. https://doi.org/10.1016/j.jmr.2012.11.023.
(22) Pinter, M.; Harter, T.; McCarthy, M.; Augustine, M. Towards Using NMR to Screen for Spoiled Tomatoes Stored in 1,000 L, Aseptically Sealed, Metal-Lined Totes. *Sensors* **2014**, *14* (3), 4167–4176. https://doi.org/10.3390/s140304167.
(23) Cooper, R. K.; Jackson, J. A. Remote Production of a Region of Homogenous Magnetic Field. *Bulletin of the American Physical Society* **1980**, *25* (1), 45-.
(24) Miller, M. N. NUMAR and NUMALOG Overview. *Concepts Magn. Reson.* **2001**, *13* (6), 379–385. https://doi.org/10.1002/cmr.1023.
(25) Kleinberg, R. L. NMR Well Logging at Schlumberger. *Concepts Magn. Reson.* **2001**, *13* (6), 396–403. https://doi.org/10.1002/cmr.1026.
(26) Prammer, M. G. NUMAR (1991-2000). *Concepts Magn. Reson.* **2001**, *13* (6), 389–395. https://doi.org/10.1002/cmr.1025.
(27) Eidmann, G.; Savelsberg, R.; Blümler, P.; Blümich, B. The NMR MOUSE, a Mobile Universal Surface Explorer. *Journal of Magnetic Resonance, Series A* **1996**, *122* (1), 104–109. https://doi.org/10.1006/jmra.1996.0185.
(28) Hugon, C.; Aubert, G.; Sakellariou, D. A Systematic Approach to the Design, Fabrication and Testing of Permanent Magnets Applied to Single-Sided NMR. In *AIP Conference Proceedings*; 2011; Vol. 1330, pp 105–108. https://doi.org/10.1063/1.3562244.
(29) Marble, A. E.; Mastikhin, I. V.; Colpitts, B. G.; Balcom, B. J. A Constant Gradient Unilateral Magnet for Near-Surface MRI Profiling. *Journal of Magnetic Resonance* **2006**, *183* (2), 228–234. https://doi.org/10.1016/j.jmr.2006.08.013.
(30) Manz, B.; Coy, A.; Dykstra, R.; Eccles, C. D.; Hunter, M. W.; Parkinson, B. J.; Callaghan, P. T. A Mobile One-Sided NMR Sensor with a Homogeneous Magnetic Field: The NMR-MOLE. *Journal of Magnetic Resonance* **2006**, *183* (1), 25–31. https://doi.org/10.1016/j.jmr.2006.07.017.
(31) Hugon, C.; Aubert, G.; Sakellariou, D. An Expansion of the Field Modulus Suitable for the Description of Strong Field Gradients in Axisymmetric Magnetic Fields: Application to Single-Sided Magnet Design, Field Mapping and STRAFI. *Journal of magnetic resonance*

(San Diego, Calif. : 1997) **2012**, *214* (1), 124–134. https://doi.org/10.1016/j.jmr.2011.10.015.
(32) Panesar, K. S.; Hugon, C.; Aubert, G.; Judeinstein, P.; Zanotti, J. M.; Sakellariou, D. Measurement of Self-Diffusion in Thin Samples Using a Novel One-Sided NMR Magnet. *Microporous and Mesoporous Materials* **2013**, *178*, 79–83. https://doi.org/10.1016/j.micromeso.2013.04.016.
(33) Judeinstein, P.; Ferdeghini, F.; Oliveira-Silva, R.; Zanotti, J.-M.; Sakellariou, D. Low-Field Single-Sided NMR for One-Shot 1D-Mapping: Application to Membranes. *Journal of Magnetic Resonance* **2017**, *277*, 25–29. https://doi.org/10.1016/j.jmr.2017.02.003.
(34) de Oliveira-Silva, R.; Bélime, A.; Le Coeur, C.; Chennevière, A.; Helary, A.; Cousin, F.; Judeinstein, P.; Sakellariou, D.; Zanotti, J.-M. Coupling NMR to SANS: Addressing at Once Structure and Dynamics in Soft Matter. *JNR* **2020**, *21* (3–4), 155–166. https://doi.org/10.3233/JNR-190114.
(35) Blümich, B.; Anferov, V.; Anferova, S.; Klein, M.; Fechete, R.; Adams, M.; Casanova, F. Simple NMR-MOUSE with a Bar Magnet. *Concepts in Magnetic Resonance Part B: Magnetic Resonance Engineering* **2002**, *15* (4), 255–261. https://doi.org/10.1002/cmr.10046.
(36) Utsuzawa, S.; Fukushima, E. Unilateral NMR with a Barrel Magnet. *Journal of Magnetic Resonance* **2017**, *282*, 104–113. https://doi.org/10.1016/j.jmr.2017.07.006.
(37) Song, Y.-Q.; Venkataramanan, L.; Hürlimann, M. D.; Flaum, M.; Frulla, P.; Straley, C. T1-T2 Correlation Spectra Obtained Using a Fast Two-Dimensional Laplace Inversion. *Journal of magnetic resonance (San Diego, Calif.: 1997)* **2002**, *154* (2), 261–268. https://doi.org/10.1006/jmre.2001.2474.
(38) Hürlimann, M. D.; Venkataramanan, L.; Flaum, C.; Speier, P.; Karmonik, C.; Freedman, R.; Heaton, N. Diffusion-Editing: New NMR Measurement of Saturation and Pore Geometry. In *SPWLA-2002-FFF*; Society of Petrophysicists and Well-Log Analysts: SPWLA, 2002; p 14.
(39) Hürlimann, M. D.; Venkataramanan, L. Quantitative Measurement of Two-Dimensional Distribution Functions of Diffusion and Relaxation in Grossly Inhomogeneous Fields. *Journal of Magnetic Resonance* **2002**, *157* (1), 31–42. https://doi.org/10.1006/jmre.2002.2567.
(40) Holz, M.; Heil, S. R.; Sacco, A. Temperature-Dependent Self-Diffusion Coefficients of Water and Six Selected Molecular Liquids for Calibration in Accurate 1H NMR PFG Measurements. *Physical Chemistry Chemical Physics* **2000**, *2* (20), 4740–4742. https://doi.org/10.1039/b005319h.
(41) Holz, M.; Mao, X.; Seiferling, D.; Sacco, A. Experimental Study of Dynamic Isotope Effects in Molecular Liquids: Detection of Translation-rotation Coupling. *The Journal of Chemical Physics* **1996**, *104* (2), 669–679. https://doi.org/10.1063/1.470863.
(42) Brownstein, K.; Tarr, C. Importance of Classical Diffusion in NMR Studies of Water in Biological Cells. *Physical Review A* **1979**, *19* (6), 2446–2453. https://doi.org/10.1103/PhysRevA.19.2446.
(43) Kleinberg, R. L.; Kenyon, W. E.; Mitra, P. P. Mechanism of NMR Relaxation of Fluids in Rock. *Journal of Magnetic Resonance, Series A* **1994**, *108* (2), 206–214. https://doi.org/10.1006/jmra.1994.1112.
(44) Mitra, P. P.; Sen, P. N.; Schwartz, L. M. Short-Time Behavior of the Diffusion Coefficient as a Geometrical Probe of Porous Media. *Physical Review B* **1993**, *47* (14), 8565–8574. https://doi.org/10.1103/PhysRevB.47.8565.

(45) Luo, Z.-X.; Paulsen, J.; Song, Y.-Q. Robust Determination of Surface Relaxivity from Nuclear Magnetic Resonance DT2 Measurements. *Journal of Magnetic Resonance* **2015**, *259*, 146–152. https://doi.org/10.1016/j.jmr.2015.08.002.